MOLECULAR AND CELLULAR BIOLOGY, May 1995, p. 2791–2799 Vol. 15, No. 5
0270-7306/95/$04.00+0


# Insulin-Stimulated Disassociation of the SOS-Grb2 Complex

STEVEN B. WATERS, KEISHI YAMAUCHI, AND JEFFREY E. PESSIN*

*Department of Physiology and Biophysics, The University of Iowa, Iowa City, Iowa 52242-1109*

Received 2 December 1994/Returned for modification 9 January 1995/Accepted 22 February 1995

**Insulin stimulation of differentiated 3T3-L1 adipocytes or Chinese hamster ovary cells expressing high levels of the insulin receptor resulted in a time-dependent decrease in the electrophoretic mobility of SOS on sodium dodecyl sulfate-polyacrylamide gels. The reduction in SOS mobility was completely reversed by alkaline phosphatase treatment, and the in vitro phosphorylation of SOS by mitogen-activated protein kinase resulted in a decrease of electrophoretic mobility identical to that following in vivo insulin stimulation. Immunoprecipitation of Grb2 followed by SOS immunoblotting demonstrated a disassociation of the SOS-Grb2 complex that paralleled the decrease in SOS electrophoretic mobility. Similarly, SOS immunoprecipitation followed by Grb2 immunoblotting also indicated an uncoupling of the SOS-Grb2 complex. Further, incubation of whole-cell extracts with glutathione-*S*-transferase–Grb2 fusion proteins demonstrated that insulin stimulation resulted in a decreased affinity of SOS for Grb2. In contrast, the disassociation of SOS from Grb2 did not affect the interactions between Grb2 and tyrosine-phosphorylated Shc. In addition to insulin, several other agents which activate the mitogen-activated protein kinase pathway (platelet-derived growth factor, serum, and phorbol ester) also resulted in the uncoupling of the SOS-Grb2 complex. Consistent with these results, expression of v-*ras* and v-*raf* resulted in a constitutive decrease in the association between SOS and Grb2. Together, these data suggest a molecular mechanism accounting for the transient activation of ras due to the uncoupling of the SOS-Grb2 complex following SOS phosphorylation.**

A common pathway for the activation of mitogen-activated protein (MAP) kinase has recently been established for several tyrosine kinase receptors including the insulin, platelet-derived growth factor (PDGF), and epidermal growth factor receptors (3, 23, 32, 34). In the case of the insulin receptor (IR), activation of the receptor intrinsic tyrosine kinase activity was originally demonstrated to enhance tyrosine phosphorylation of a 185-kDa protein termed IRS1 for IR substrate 1 (22, 47, 51). IRS1 contains multiple tyrosine phosphorylation acceptor sites which, when phosphorylated, create specific recognition motifs for src homology 2 (SH2) domain-containing proteins (55). These include the p85 regulatory subunit of the phosphatidylinositol 3-kinase, the protein tyrosine-specific phosphatase Syp, and the small adaptor proteins Nck and Grb2 (26, 46).

In addition to IRS1, the SH2 domain-containing α2 collagen-related proteins (Shc) have been identified as proximal targets for several growth factor tyrosine kinases, including the IR (38). The Shc family consists of three related proteins, with the 46- and 52-kDa species resulting from alternative usage of two distinct translation initiation sites within the same transcript and the 66-kDa species most likely arising from an alternatively spliced message (36). In contrast to IRS1, the Shc proteins are tyrosine phosphorylated on a single tyrosine residue (Y-317) which serves as a docking site for Grb2 (41, 45). Grb2 was originally identified as a 23-kDa-growth factor receptor-binding protein which contains a single SH2 domain flanked by two src homology 3 (SH3) domains (29). The SH3 domains of Grb2 direct the association with several proteins containing proline-rich motifs, including the 150-kDa guanylnucleotide exchange factor for ras, termed SOS for the *Drosophila melanogaster* gene Son-of-Sevenless (7, 30, 42, 43, 50).

In contrast, ras inactivation is regulated by a ras GTPase-activating protein (rasGAP) which stimulates the hydrolysis of the GTP-bound ras to the GDP-bound state (48). Thus, the dynamic equilibrium between SOS and rasGAP activities within a cell defines the relative activation state of ras. Although rasGAP is a potential target for regulation, insulin treatment does not have any significant effect on rasGAP phosphorylation, activity, and/or localization (11). However, several studies have demonstrated that, in unstimulated cells, SOS constitutively associates with Grb2, whereas following insulin stimulation the SOS-Grb2 complex becomes associated with Shc (37, 44, 45) and perhaps IRS1 (4, 45). Thus, the targeting and/or activation of SOS guanylnucleotide exchange activity by its indirect association with Shc via the small adaptor protein Grb2 results in the increased conversion of ras from the inactive GDP-bound state to the active GTP-bound form (2, 39).

Although the above mechanism can account for the rapid increase in ras GTP loading, tyrosine kinase growth factor stimulation results in a transient activation of ras. In most systems, maximum levels of GTP-bound ras are observed approximately 10 min following growth factor stimulation and return to basal (35) or near-basal levels within 60 min (16, 19, 53). Thus, a feedback mechanism(s) which inhibits the Grb2-SOS activation signal and/or stimulates rasGAP activity within a similar time frame must also exist. In the present paper, we demonstrate that insulin and several other agents which also activate the MAP kinase pathway generate a feedback cascade which results in the disassociation of the SOS-Grb2 complex. The uncoupling of the SOS-Grb2 complex may provide a molecular mechanism accounting for the transient activation of ras following insulin stimulation.

## MATERIALS AND METHODS

**Cell culture.** Chinese hamster ovary (CHO) cells expressing $3 \times 10^6$ human (IRs) were grown in alpha-minimal essential medium containing nucleotides, 100 U of penicillin per ml, 100 μg of streptomycin per ml, and 10% fetal bovine serum. 3T3-L1 fibroblasts were maintained in Dulbecco's modified Eagle's medium containing penicillin-streptomycin as above plus 10% calf serum and incubated at 37°C in an 8% $CO_2$–air gas mixture. 3T3-L1 fibroblasts (2 days postconfluent) were differentiated into adipocytes by replacing the medium with Dulbecco's modified Eagle's medium containing penicillin-streptomycin, 10% fetal bovine serum, 0.25 μM dexamethasone, 500 μM isobutylmethylxanthine,

* Corresponding author. Mailing address: Department of Physiology and Biophysics, The University of Iowa, Iowa City, IA 52242-1109.

and 1 μg of insulin per ml for 3 days. The 3T3-L1 cells were then incubated with Dulbecco's modified Eagle's medium containing 100 U of penicillin per ml, 100 μg of streptomycin per ml, and 10% fetal bovine serum for 8 to 40 days to maintain the adipocyte phenotype. Prior to experiments, both the 3T3-L1 adipocytes and CHO-IR cells were incubated with serum-free medium containing 0.5% bovine serum albumin for 16 h. The cells were then treated with or without various hormones for the times indicated in each figure legend. Treatments were stopped by rapidly removing the medium and freezing the cells with liquid nitrogen. Whole-cell lysates were prepared by thawing cells (10-cm plate) in 1 ml of 1% Triton X-100 lysis buffer (50 mM HEPES, [*N*-2-hydroxyethylpiperazine-*N*′-2-ethanesulfonic acid], [pH 7.8], 1% Triton X-100, 2.5 mM EDTA, 100 mM sodium fluoride, 10 mM sodium $PP_i$, 2 mM sodium vanadate, 1 mM phenylmethylsulfonyl fluoride, 2 μM pepstatin, 0.5 trypsin inhibitory units of aprotinin, and 10 μM leupeptin) for 30 min at 4°C. Insoluble material was removed by centrifugation at 12,000 × *g* for 15 min at 4°C, and the total protein in the supernatant was determined by the method of Bradford.

**Immunoblotting.** Whole-cell lysates or immunoprecipitates were separated on reducing sodium dodecyl sulfate (SDS)–5 to 10% polyacrylamide gradient gels and transferred to polyvinylidene difluoride membranes with 1 A for 2 h at 4°C. Immunoblotting of the whole-cell lysates was performed with a SOS polyclonal antibody (αSOS; Upstate Biotechnology Inc.). Immunoblotting of immunoprecipitates was done with a SOS monoclonal antibody (Transduction Laboratories), a Grb2 monoclonal antibody (αGrb2; Transduction Laboratories), a Shc monoclonal antibody (αShc; Transduction Laboratories), or a monoclonal phosphotyrosine antibody, PY20-HRP (αPY; Santa Cruz Biotechnology). The primary monoclonal and polyclonal antibodies (except PY20-HRP) were detected with horseradish peroxidase-conjugated anti-rabbit or anti-mouse immunoglobulin G (IgG), respectively (Bio-Rad) and visualized by the enhanced chemiluminescence detection system (Amersham).

**Immunoprecipitation.** Whole-cell lysates were prepared as described above. SOS and Grb2 were immunoprecipitated from the lysates by incubation with either αSOS (Santa Cruz Biotechnology) or αGrb2 (Santa Cruz Biotechnology) for 2 h at 4°C. The resultant immune complexes were precipitated by incubation with protein A-agarose for 1 h at 4°C. Samples for immunoblotting were washed three times with Tris-buffered saline (20 mM Tris [pH 7.6], 150 mM NaCl), resuspended in SDS-sample buffer (125 mM Tris-HCl [pH 6.8], 20% [vol/vol] glycerol, 4% [wt/vol] SDS, 100 mM dithiothreitol, 0.1% [wt/vol] bromphenol blue), heated at 100°C for 5 min, and immunoblotted as indicated above.

**In vitro phosphorylation-dephosphorylation of SOS.** The dephosphorylation of SOS was performed with αSOS immunoprecipitates from whole-cell lysates of control or insulin-stimulated cells. Briefly, the αSOS immunoprecipitates were washed twice with lysis buffer and twice with alkaline phosphatase buffer (20 mM HEPES [pH 7.4], 100 mM NaCl, 1 mM dithiothreitol, 1 mM $MgCl_2$, and 0.1 mM $ZnCl_2$, 1 mM phenylmethylsulfonyl fluoride, 0.5 trypsin inhibitory units of aprotinin per ml, and 10 μM leupeptin). The samples were incubated with 25 U of calf intestinal phosphatase (Sigma Chemical Co.) in a total volume of 200 μl for 60 min at room temperature. The samples were then washed three times with phosphate- buffered saline, solubilized in SDS-sample buffer, and immunoblotted with αSOS as described above.

In vitro MAP kinase phosphorylation was performed on the αSOS immunoprecipitates with partially purified MAP kinase provided by Melanie Cobb, University of Texas, Dallas (6). Briefly, the immunoprecipitates were washed three times with phosphate-buffered saline and once with MAP kinase assay buffer (30 mM HEPES [pH 8.0], 1 mM ATP, 1 mM dithiothreitol, 1 mM sodium vanadate, 10 mM $MgCl_2$, and 100 μg of bovine serum albumin per ml). The immunoprecipitates were resuspended in 100 μl of the MAP kinase assay buffer, and the reaction was initiated by the addition of 12 μl of partially purified MAP kinase. After a 60-min incubation at room temperature, the assay was terminated by the addition of SDS-sample buffer and heating at 100°C for 5 min.

**Precipitation of SOS with a GST-Grb2 fusion protein.** Human Grb2 was cloned by reverse transcriptase-PCR with brain RNA (Clontech), and the isolated cDNA sequence was confirmed by sequence analysis. The hGrb2 cDNA was subcloned into pGEX-3X (Pharmacia Biotech) and isolated according to the manufacturer's instructions. The glutathione-*S*-transferase (GST)–hGrb2 fusion protein (0, 1, 3, 10, 30, or 100 μg) was diluted in phosphate-buffered saline containing 1 mg of bovine serum albumin per ml and incubated for 1 h at 4°C with glutathione-Sepharose (25-μl bed volume). The glutatione-Sepharose-bound GST-Grb2 fusion protein was then incubated for 1 h at 4°C with whole-cell lysates (50 mM HEPES [pH 7.8], 1% Triton X-100, 2.5 mM EDTA, 100 mM sodium fluoride, 10 mM sodium $PP_i$, 2 mM sodium vanadate, 1 mM phenylmethylsulfonyl fluoride, 2 μM pepstatin, 0.5 trypsin inhibitory units of aprotinin, and 10 μM leupeptin) isolated from either unstimulated or 100 nM insulin-stimulated 3T3-L1 adipocytes for 15 min. The Sepharose beads were pelleted and washed three times with phosphate-buffered saline and solubilized in SDS-sample buffer. The amount of SOS associated with the immobilized GST-hGrb2 fusion protein was determined by immunoblotting with αSOS.

In an alternative approach, the detergent cell lysates (50 mM HEPES [pH 7.8], 1% Triton X-100, 2.5 mM EDTA, 100 mM sodium fluoride, 10 mM sodium $PP_i$, 2 mM sodium vanadate, 1 mM phenylmethylsulfonyl fluoride, 2 μM pepstatin, 0.5 trypsin inhibitory units of aprotinin, and 10 μM leupeptin) from control and insulin-stimulated CHO-IR cells were incubated with various concentrations of purified GST-Grb2 fusion protein as described above. The samples were then immunoprecipitated with the αSOS monoclonal antibody, washed, and immunoblotted for Grb2. The identical detergent lysates from control and insulin-stimulated CHO-IR cells were also immunoprecipitated with the αSOS monoclonal antibody, washed, and incubated with various concentrations of purified GST-Grb2 fusion protein in the 1% Triton X-100 whole-cell lysis buffer. Following a 3-h incubation at 4°C, the samples were washed in Tris-buffered saline and immunoblotted for the presence of GST-Grb2.

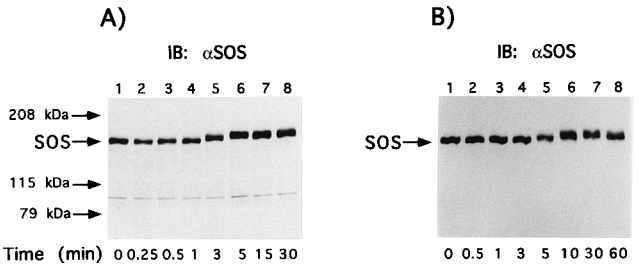


FIG. 1. Insulin stimulation decreases the electrophoretic mobility of SOS in a time-dependent manner. CHO-IR cells (A) and 3T3-L1 adipocytes (B) were incubated with 100 nM insulin for the various times indicated in the figure. Whole-cell lysates were prepared as described in Materials and Methods and immunoblotted with an antibody directed against SOS (αSOS). IB, immunoblot.

**Quantitative transient transfection by electroporation.** We have recently demonstrated that electroporation can be used to express various cDNAs in CHO-IR cells with 85 to 100% transfection efficiency (52). Briefly, CHO-IR cells were electroporated with a total of 40 μg of plasmid DNA at 340 V and 960 μF in 500 μl of phosphate-buffered saline. Following electroporation, the cells were plated in alpha-minimal essential medium containing 10% serum, and cell debris was removed by replacement with fresh media 12 h later. Under these conditions, approximately 25% of the cells remained viable, and of these, 85 to 100% expressed the protein of interest, depending upon the particular experiment. The constitutively active v-*ras* (pMV7-v*ras*) and v-*raf* (pZipneo-v*raf*) were obtained from Gary Johnson (The National Jewish Center for Immunology and Respiratory Medicine, Denver, Colo.).

## RESULTS

**Insulin decreases the electrophoretic mobility of SOS.** The carboxyl-terminal domain of the ras guanylnucleotide exchange factor SOS contains several potential MAP kinase phosphorylation sites (42), suggesting that SOS may be a direct substrate for MAP kinase. In this regard, incubation of SOS with MAP kinase in vitro results in the serine/threonine phosphorylation of SOS and a characteristic reduction in the electrophoretic mobility of SOS (9). To determine whether SOS is phosphorylated by insulin stimulation in vivo, we examined the effect of insulin treatment on the SDS-polyacrylamide gel electrophoretic mobility of SOS in CHO-IR and 3T3-L1 adipocytes (Fig. 1). Insulin stimulation of both cell types resulted in a time-dependent reduction in the electrophoretic mobility of SOS. In CHO-IR cells, there was no effect on SOS mobility following treatment with insulin for times of up to 1 min (Fig. 1A, lanes 1 to 4). However, a decrease in SOS mobility was detected following 3 min of insulin treatment, with a maximal effect reached by 5 min (Fig. 1A, lanes 5 and 6). The SOS electrophoretic mobility shift remained persistent for at least 30 min and was apparently quantitative, as only a single SOS immunoreactive band was detected at each time point (Fig. 1A, lanes 7 and 8). Similarly, in response to insulin treatment 3T3-L1 adipocytes also displayed a quantitative reduction in SOS electrophoretic mobility (Fig. 1B). However, it should be noted that in 3T3-L1 adipocytes the time dependence of the SOS gel shift was slower than in CHO-IR cells. In the 3T3-L1 adipocytes, the decrease in SOS mobility was initially detected following 5 min of insulin stimulation (Fig. 1B, lane 5) and was maximal by 10 min (Fig. 1B, lane 6). The slightly slower time course in 3T3-L1 adipocytes compared with the CHO-IR cells

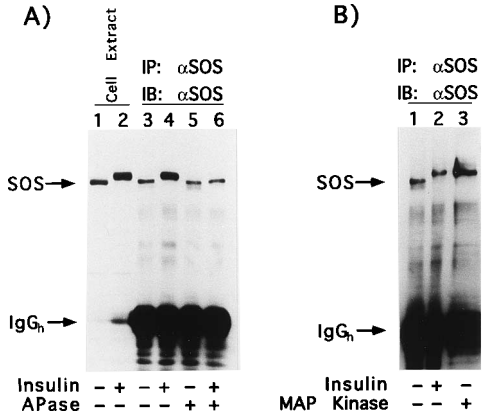


FIG. 2. The insulin-stimulated decrease in SOS mobility results from serine/threonine phosphorylation. (A) CHO-IR cells were incubated in the absence (lanes 1, 3, and 5) or presence (lanes 2, 4, and 6) of 100 nM insulin for 10 min. Whole-cell lysates from control (lane 1) and insulin-stimulated (lane 2) cells were immunoblotted with αSOS. SOS was immunoprecipitated from the same whole-cell lysates (lanes 3 to 6) and incubated in the absence (lanes 3 and 4) or presence (lanes 5 and 6) of alkaline phosphatase as described in Materials and Methods. The immunoprecipitates were then subjected to SDS-polyacrylamide gel electrophoresis and immunoblotted with an antibody directed against SOS (αSOS). (B) CHO-IR cells were incubated in the absence (lanes 1 and 3) or presence (lane 2) of 100 nM insulin for 10 min. SOS was immunoprecipitated from the whole-cell lysates and incubated in the absence (lanes 1 and 2) or presence (lane 3) of Mg-ATP plus partially purified MAP kinase as described in Materials and Methods. The immunoprecipitates were then subjected to SDS-polyacrylamide gel electrophoresis and immunoblotted with an antibody directed against SOS (αSOS). $IgG_h$ indicates the relative mobility of the immunoglobulin G heavy chain. APase, alkaline phosphatase; IP, immunoprecipitation; IB, immunoblot.

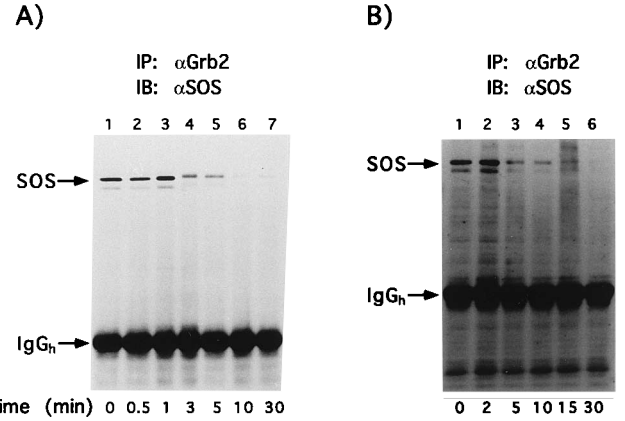


FIG. 3. Insulin stimulation decreases the amount of SOS associated with Grb2 in a time-dependent manner. CHO-IR cells (A) and 3T3-L1 adipocytes (B) were incubated with 100 nM insulin for various times as indicated in the figure. Whole-cell lysates were prepared and immunoprecipitated with the Grb2 antibody (αGrb2) as described in Materials and Methods. The immunoprecipitates were then subjected to SDS-polyacrylamide gel electrophoresis and immunoblotted with an antibody directed against SOS (αSOS). $IgG_h$ indicates the relative mobility of the immunoglobulin G heavy chain. The band located immediately below the major SOS immunoreactive material represents an SOS proteolytic fragment that occurred in this particular experiment. IP, immunoprecipitation; IB, immunoblot.

probably reflects the lower level of IR expression in the adipocytes (14, 25).

In addition, we consistently observed greater αSOS immunoreactivity in whole-cell detergent extracts from stimulated cells than in those from unstimulated controls (Fig. 1; see also Fig. 2, 8, and 9). Since this difference was detected with several αSOS antibodies (data not shown) and was reversible with alkaline phosphatase treatment (see Fig. 2), this suggests that the shifted SOS protein from insulin-stimulated cells was more efficiently transferred to the polyvinylidene difluoride membranes than the SOS protein from unstimulated cells.

**Serine/threonine phosphorylation of SOS is responsible for the decrease in electrophoretic mobility.** To determine whether the apparent SOS electrophoretic mobility shift was due to phosphorylation, we isolated SOS by specific immunoprecipitation from control and insulin-stimulated CHO-IR cells (Fig. 2). As previously observed, whole-cell extracts from insulin-stimulated CHO-IR cells displayed the characteristic decrease in SOS mobility (Fig. 2A, lane 2) compared with control cell extracts (Fig. 2A, lane 1). Similarly, cell extracts immunoprecipitated with an SOS-specific antibody (αSOS) also demonstrated the decrease in SOS mobility following in vivo insulin stimulation (Fig. 2A, lanes 3 and 4). However, incubation of immunoprecipitated SOS from control cell extracts (Fig. 2A, lane 5) or insulin-stimulated cells (Fig. 2A, lane 6) with alkaline phosphatase reversed the effect of in vivo insulin treatment on the electrophoretic mobility of SOS. These data indicate that the decrease in SOS mobility following insulin stimulation resulted from increased phosphorylation of SOS. In addition, phosphotyrosine immunoblotting of the immunoprecipitated SOS did not detect any phosphotyrosine phosphorylation (data not shown), suggesting that the insulin-stimulated phosphorylation occurred on serine and/or threonine residues.

Since the carboxyl-terminal region of SOS contains seven consensus MAP kinase phosphorylation sites, we examined the ability of MAP kinase to phosphorylate SOS in vitro (Fig. 2B). Immunoprecipitation of SOS from insulin-treated CHO-IR cells displayed the expected reduction in SOS mobility (Fig. 2B, lane 2) compared with SOS immunoprecipitated from unstimulated cells (Fig. 2B, lane 1). Incubation of the SOS immunoprecipitate from unstimulated cells with MAP kinase and Mg-ATP decreased the mobility of SOS (Fig. 2B, lane 3). The decreased SOS mobility resulting from MAP kinase phosphorylation in vitro was equivalent to that observed for SOS immunoprecipitated from in vivo insulin-stimulated cells. Taken together, these data suggest that the insulin-stimulated decrease in SOS electrophoretic mobility in vivo could have resulted from a MAP kinase-mediated serine/threonine phosphorylation event.

**Insulin stimulation uncouples SOS from Grb2.** It has been established that, in unstimulated cells, SOS is bound to Grb2 via direct binding interactions between the proline-rich carboxyl-terminal domain of SOS and the SH3 domains of Grb2 (8, 12, 28, 40). We therefore examined the possibility that the serine/threonine phosphorylation of SOS might alter the binding interaction between SOS and Grb2 (Fig. 3). In the absence of insulin, immunoprecipitation of CHO-IR cell extracts with a Grb2-specific antibody (αGrb2) resulted in the coimmunoprecipitation of SOS as detected by αSOS immunoblotting (Fig. 3A, lane 1). Essentially identical amounts of coimmunoprecipitated SOS were detected in the αGrb2 immunoprecipitates following insulin treatment from 30 s to 1 min (Fig. 3A, lanes 2 and 3). However, 3 min of insulin stimulation resulted in a significant decrease in the ability of the Grb2 antibody to coimmunoprecipitate SOS (Fig. 3A, lane 4), and by 10 to 30 min, there was virtually no detectable SOS in the Grb2 immunoprecipitates (Fig. 3A, lanes 6 and 7). Similarly, immunoprecipitation of Grb2 from unstimulated 3T3-L1 adipocyte extracts resulted in the coimmunoprecipitation of SOS (Fig. 3B, lane 1), which was unaffected by short-term (2-min) insulin treatment (Fig. 3B, lane 2). Consistent with the CHO-IR cells, incubation of 3T3-L1 adipocytes with insulin for longer times

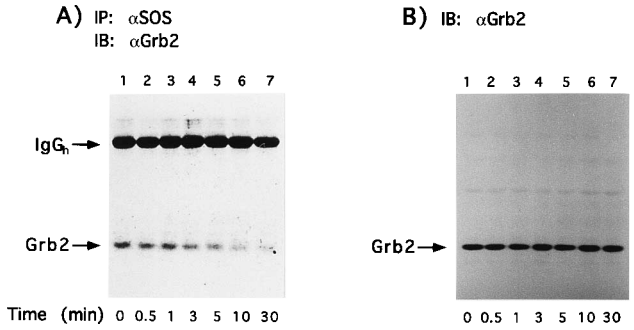


FIG. 4. Insulin stimulation decreases the amount of Grb2 associated with SOS in a time-dependent manner. (A) CHO-IR cells were incubated with 100 nM insulin for various times as indicated in the figure. Whole-cell lysates were prepared and SOS was immunoprecipitated with the SOS antibody (αSOS) as described in Materials and Methods. The immunoprecipitates were then immunoblotted with an antibody directed against Grb2 (αGrb2). (B) CHO-IR cell extracts obtained in panel A were immunoblotted with the Grb2 antibody (αGrb2). $IgG_h$ indicates the relative mobility of the immunoglobulin G heavy chain. IP, immunoprecipitation; IB, immunoblot.

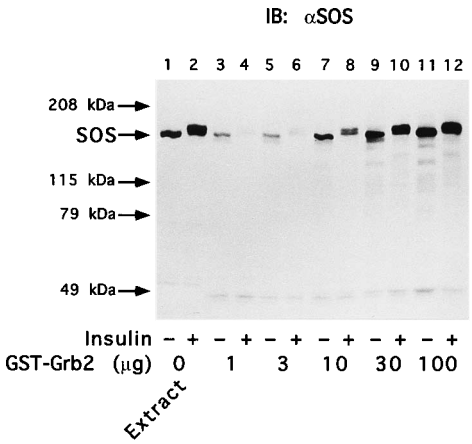


FIG. 5. Insulin-stimulated disassociation of the SOS-Grb2 complex determined by precipitation with a GST-Grb2 fusion protein. 3T3-L1 adipocyte extracts were prepared from control cells (lanes 1, 3, 5, 7, 9, and 11) and cells incubated with 100 nM insulin for 15 min (lanes 2, 4, 6, 8, 10, and 12). The cell extracts were either used directly for immunoblotting (lanes 1 and 2) or incubated for an additional 1 h with increasing amounts of the GST-hGrb2 fusion protein (lanes 3 to 12) as indicated in the figure. The samples were then precipitated, subjected to SDS-polyacrylamide gel electrophoresis, and immunoblotted with an αSOS antibody as described in Materials and Methods. IB, immunoblot.

(5 to 15 min) resulted in a reduction of Grb2-immunoprecipitated SOS protein (Fig. 3B, lanes 3, 4, and 5) with essentially no detectable SOS in the Grb2 immunoprecipitate by 30 min (Fig. 3B, lane 6). The decreased amount of SOS coimmunoprecipitated with the Grb2 antibody following insulin stimulation was not the result of alterations in the total cellular content of SOS protein (Fig. 1).

Having observed an uncoupling of SOS-Grb2 interaction by Grb2 immunoprecipitation, we next determined the ability of an SOS-specific antibody to coimmunoprecipitate Grb2 (Fig. 4). Consistent with Fig. 3, insulin treatment of CHO-IR cells resulted in a time-dependent decrease in the ability of the SOS antibody (αSOS) to coimmunoprecipitate Grb2 (Fig. 4A). Immunoblotting of whole-cell extracts with the Grb2 antibody also demonstrated that there was no significant alteration in the amount of expressed Grb2 protein under these conditions (Fig. 4B). Thus, insulin stimulation apparently caused a disassociation of SOS from Grb2 which roughly parallels the time-dependent decrease in SOS electrophoretic mobility. The inability to coimmunoprecipitate SOS with Grb2 following insulin treatment appears to result from decreased interactions between SOS and Grb2 and not from alterations in the expression levels of SOS or Grb2 protein.

**In vitro disassociation of the SOS-Grb2 complex.** Although the disassociation of the SOS-Grb2 complex was detected by immunoprecipitation of cell extracts with both αSOS and αGrb2 antibodies, it is still formally possible that these antibodies were detecting an insulin-stimulated change in the conformation of SOS and Grb2 and not necessarily a physical separation of SOS from Grb2. Therefore, as an alternative approach, SOS was precipitated from 3T3-L1 adipocyte whole-cell extracts with a bacterially expressed GST-Grb2 fusion protein (Fig. 5). As specific markers, 3T3-L1 adipocyte extracts from unstimulated and insulin-stimulated cells were directly subjected to αSOS immunoblotting (Fig. 5, lanes 1 and 2). Incubation of the unstimulated cell extracts with 1 or 3 μg of immobilized GST-Grb2 (Fig. 5, lanes 3 and 5) demonstrated the specific binding of SOS whereas the extracts from insulin-stimulated cells displayed reduced SOS binding (Fig. 5, lanes 4 and 6). Although a differential precipitation of SOS from control and insulin-stimulated cells was still detected with 10 μg of GST-Grb2 (Fig. 5, lanes 7 and 8), approximately equal amounts of SOS were precipitated with 30 μg of immobilized GST-Grb2 (Fig. 5, lanes 9 and 10). Further, incubation of the cell extracts with higher amounts (100 μg) of GST-Grb2 was essentially saturating (Fig. 5, lanes 11 and 12) and resulted in the complete precipitation of SOS from the cell extracts (data not shown). These data demonstrate that an insulin-dependent decrease in SOS-Grb2 interaction was recapitulated in cell extracts and was not a result of differential antibody reactivity. Moreover, the GST-Grb2 dose dependence of SOS binding demonstrates that the decreased extent of SOS-Grb2 association resulted from a reduction in specific binding affinity without any significant effect on SOS protein levels.

In an alternative approach to examine the in vitro interaction of SOS with Grb2, extracts from control and insulin-stimulated CHO-IR cells were incubated with various concentrations of the GST-Grb2 fusion protein for 3 h at 4°C (Fig. 6). The extracts were immunoprecipitated with αSOS, and the resulting immunoprecipitates were immunoblotted for the presence of the 52-kDa GST-Grb2 fusion protein (Fig. 6A). As expected, incubation of the detergent extracts from control cells with low concentrations of the GST-Grb2 fusion protein (0.3 and 1 μg/ml) resulted in a significantly greater association with SOS than the GST-Grb2 incubated with extracts from insulin-stimulated cells (Fig. 6A, lanes 1 to 4). Consistent with Fig. 5, incubation with higher GST-Grb2 concentrations (3 and 10 μg/ml) failed to demonstrate any difference in SOS association between control and insulin-stimulated cell extracts (Fig. 6A, lanes 5 to 8).

Surprisingly, however, a different result was obtained when GST-Grb2 was incubated with washed αSOS immunoprecipitates (Fig. 6B). At all GST-Grb2 concentrations examined (0.3 to 10 μg/ml), no significant difference in the amount of Grb2 binding was observed between SOS immunoprecipitated from extracts of control cells and that from extracts of insulin-stimulated cells (Fig. 6B, lanes 1 to 8). Essentially identical results were obtained when SOS was immunoprecipitated with either an amino-terminal αSOS antibody or a carboxy-terminal αSOS antibody (data not shown). Together, these data indicate that the reduced binding of Grb2 to SOS isolated from insulin-stimulated cells requires the presence of an additional factor(s)

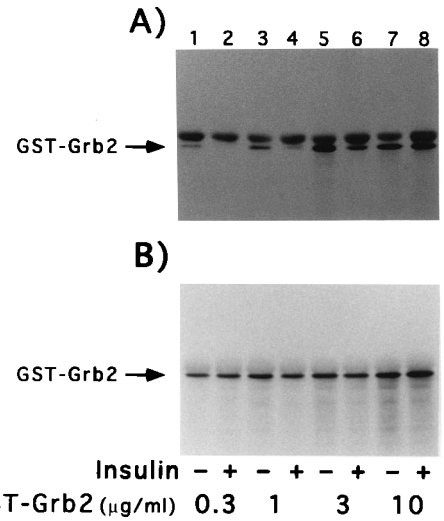


FIG. 6. Insulin-stimulated disassociation of the SOS-Grb2 complex occurs in whole-cell detergent lysates but not after immunoprecipitation with an αSOS antibody. CHO-IR detergent cell extracts were prepared from control cells (lanes 1, 3, 5, and 7) and cells incubated with 100 nM insulin for 15 min (lanes 2, 4, 6, and 8). (A) These cell extracts were incubated with 0.3 (lanes 1 and 2), 1 (lanes 3 and 4), 3 (lanes 5 and 6), and 10 (lanes 7 and 8) μg of purified GST-Grb2 per ml for 3 h at 4°C. The samples were then immunoprecipitated with the αSOS antibody and immunoblotted for the presence of the 52-kDa GST-Grb2 fusion protein as described in Materials and Methods. (B) The identical detergent cell extracts prepared in panel A were immunoprecipitated with the αSOS antibody and subsequently incubated with GST-Grb2 under the identical conditions. The samples were then immunoblotted for the presence of GST-Grb2.

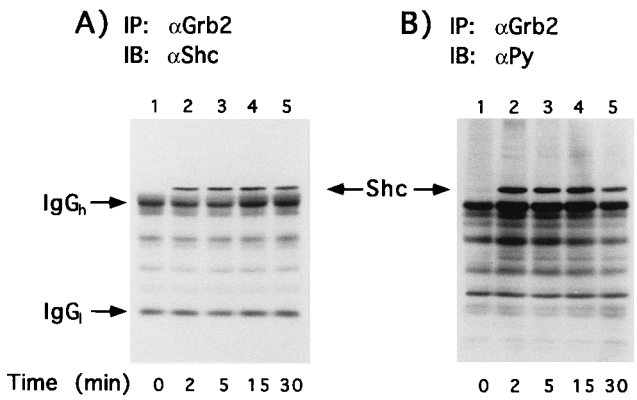


FIG. 7. Insulin-stimulated disassociation of the SOS-Grb2 complex does not affect the interaction between Shc and Grb2. CHO-IR cells were incubated in the absence (lane 1) or presence (lanes 2 to 5) of 100 nM insulin for various times as indicated in the figure. Whole-cell lysates were prepared and immunoprecipitated with the Grb2 antibody (αGrb2) as described in Materials and Methods. The immunoprecipitates were then subjected to SDS-polyacrylamide gel electrophoresis and immunoblotted with either the Shc antibody (αShc) (A) or the phosphotyrosine antibody PY20-HRP (αPy) (B). $IgG_h$ and $IgG_l$ indicate the relative mobilities of the immunoglobulin G heavy and light chains, respectively. IP, immunoprecipitation; IB, immunoblot.

which was probably removed during the washing of the αSOS immunoprecipitates.

**Disassociation of SOS-Grb2 binding does not affect insulin-stimulated Shc-Grb2 association.** In addition to the SH3 domains of Grb2 binding to the carboxyl-terminal proline-rich region of SOS, the Grb2 SH2 domain directs association with tyrosine-phosphorylated Shc (8, 12, 40, 44). In this manner, Grb2 functions as an adaptor protein linking SOS to tyrosine-phosphorylated Shc. Since insulin stimulation resulted in the disassociation of SOS from Grb2, we next examined the association of Grb2 with Shc (Fig. 7). As expected, there was no detectable Shc protein in αGrb2 immunoprecipitates from CHO-IR cell extracts prepared from unstimulated cells (Fig. 7A, lane 1). However, following 2 min of insulin stimulation, the 52-kDa form of Shc was readily detected in the αGrb2 immunoprecipitate (Fig. 7A, lane 2). The relative amount of αGrb2-immunoprecipitated Shc protein remained essentially unchanged after from 2 to 30 min of insulin stimulation (Fig. 7A, lanes 2 to 5). The insulin-dependent tyrosine phosphorylation of Shc was also confirmed by phosphotyrosine blotting of the αGrb2 immunoprecipitates (Fig. 7B). Only the tyrosine-phosphorylated 52-kDa Shc species was coimmunoprecipitated with the αGrb2 antibody following insulin stimulation (Fig. 7B, lanes 1 and 2). The amount of Grb2 associated with tyrosine-phosphorylated Shc also remained constant over the same time period in which SOS was completely disassociated from Grb2 (Fig. 7B, lanes 3 to 5). In addition to Shc and SOS, Grb2 also directly binds the microtubule-associated protein dynamin (17, 20). As observed for Shc, insulin treatment had no effect on the amount of dynamin coimmunoprecipitated with αGrb2 in the same cell extracts that displayed reduced αGrb2 antibody-coimmunoprecipitated SOS (data not shown).

**Persistent activation of the MAP kinase pathway disassociates the SOS-Grb2 complex.** To further characterize the signaling pathway mediating the insulin-stimulated disassociation of the SOS-Grb2 complex, we persistently activated the MAP kinase pathway by expression of constitutively active mutants of ras and raf. We have recently developed a transient electroporation protocol which results in a high level of transfection efficiency suitable for cell biological studies (52). Although the efficiency of transfection depends upon the particular cell type, 85 to 100% of electroporated CHO-IR cells express the cDNA of interest. We therefore utilized this method to examine the effect of ras and raf activation on SOS-Grb2 interactions. As previously observed in nontransfected CHO-IR cells, insulin stimulation resulted in a decrease of SOS electrophoretic mobility (Fig. 8A, lanes 1 and 2) and disassociation from Grb2 (Fig. 8B, lanes 1 and 2). Expression of constitutively active ras (v-*ras*) or raf (v-*raf*) mutants resulted in a partial decrease in SOS electrophoretic mobility (Fig. 8A, lanes 3 and 5), which was further retarded by treatment with 100 nM insulin for 15 min (Fig. 8A, lanes 4 and 6). In parallel, expression of v-*ras* or v-*raf* resulted in a partial reduction in the amount of αGrb2-immunoprecipitated SOS protein (Fig. 8B, lanes 3 and 5) compared with unstimulated cell extracts (Fig. 8B, lane 1). Subsequently, insulin stimulation further enhanced the disassociation of the SOS-Grb2 complex to below detectable levels (Fig. 8B, lanes 4 and 6). These data demonstrate that persistent activation of downstream signaling pathways, independent of tyrosine kinase receptor activation, decreased the amount of SOS associated with Grb2.

**Heterologous ligand stimulation uncouples SOS-Grb2 binding.** Since the persistent activation of ras or raf resulted in the phosphorylation of SOS and the disassociation of the SOS-Grb2 complex, we speculated that other ligands and/or pathways that activate MAP kinase would also induce the disassociation of the SOS-Grb2 complex. To test this hypothesis, we examined the effect of several agents known to stimulate the MAP kinase cascade via activation of the ras-raf pathway. Incubation of quiescent CHO-IR cells with 100 nM insulin, 15% serum, 50 ng of PDGF-BB, or 100 nM 12-*O*-tetradecanoylphorbol-13-myristic acid (TPA) resulted in the characteristic electrophoretic mobility shift of SOS (Fig. 9A, lanes 2 to 5) compared with unstimulated cells (Fig. 9A, lanes 1 and 6).

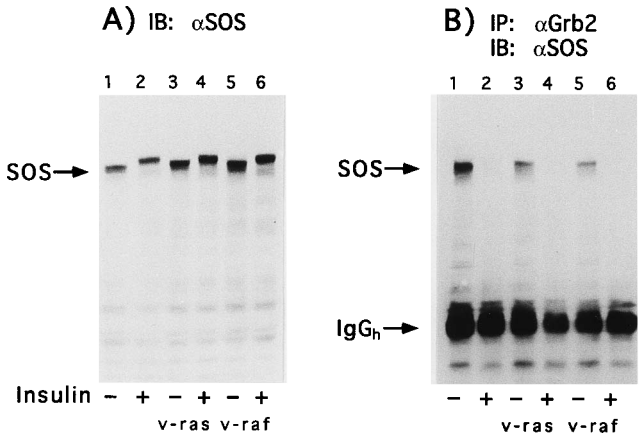


FIG. 8. Disassociation of the SOS-Grb2 complex by expression of v-*ras* and v-*raf*. CHO-IR cells were transiently transfected by quantitative electroporation with an empty vector (lanes 1 and 2) or with either the v-*ras* (lanes 3 and 4) or v-*raf* (lanes 5 and 6) expression plasmids as described in Materials and Methods. Forty-eight hours following transfection, the cells were incubated in the absence (lanes 1, 3, and 5) or presence (lanes 2, 4, and 6) of 100 nM insulin for 15 min. (A) Whole-cell extracts were subjected to SDS-polyacrylamide gel electrophoresis and immunoblotted with the SOS antibody (αSOS). (B) In parallel, the whole-cell extracts were immunoprecipitated with the Grb2 antibody (αGrb2), and the immunoprecipitates were subjected to SDS-polyacrylamide gel electrophoresis and immunoblotted with an antibody directed against SOS (αSOS). $IgG_h$ indicates the relative mobility of the immunoglobulin G heavy chain. IB, immunoblot; IP, immunoprecipitation.

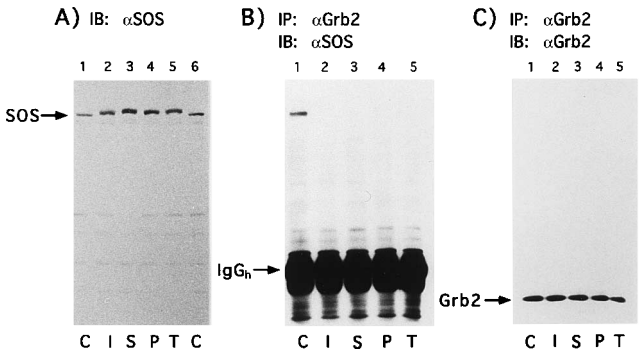


FIG. 9. Various activators of the MAP kinase pathway result in SOS phosphorylation and the disassociation of the SOS-Grb2 complex. CHO-IR cells were incubated in the absence (C; lanes 1 and lane 6 in panel A) or presence of 100 nM insulin (I; lanes 2), 15% serum (S; lanes 3), 50 ng of PDGF-BB (P; lanes 4), or 100 nM TPA (T; lanes 5) for 15 min. (A) Whole-cell extracts were subjected to SDS-polyacrylamide gel electrophoresis and immunoblotted with the SOS antibody (αSOS) as described in Materials and Methods. (B) The extracts were immunoprecipitated with the Grb2 antibody (αGrb2), and the immunoprecipitates were then immunoblotted with an antibody directed against SOS (αSOS). (C) The polyvinylidene difluoride membrane used in panel B was stripped and reprobed with the αGrb2 antibody. $IgG_h$ indicates the relative mobility of the immunoglobulin G heavy chain. IB, immunoblot; IP, immunoprecipitation.

In parallel, these treatments also induced the disassociation of the SOS-Grb2 complex as determined by the decreased amount of αGrb2-coimmunoprecipitated SOS protein (Fig. 9B, lanes 2 to 5) compared with the untreated control cell extract (Fig. 9B, lane 1). Further, this disassociation of the SOS-Grb2 complex occurred without any significant change in the amount of SOS protein expression (Fig. 9A) or in the amount of immunoprecipitated Grb2 protein (Fig. 9C).

## DISCUSSION

Numerous studies have demonstrated that ras plays a central role in the conversion of tyrosine kinase activity to serine/threonine kinase-mediated events. For example, it has been directly demonstrated that the c-raf1 kinase associates with ras in the active GTP-bound state (24, 33, 54). Further, raf functions as at least one upstream kinase for the dual specificity kinase MEK, which phosphorylates and stimulates MAP kinase activity (3, 5). The activation of MAP kinase then provides an important bifurcation point for the regulation of metabolic, transcriptional, and mitogenic events (10).

In addition to this downstream pathway, at least one upstream pathway leading to the activation of ras by tyrosine kinase receptors has been established. All receptor tyrosine kinases examined to date result in the tyrosine phosphorylation of Shc, which then specifically associates with the SH2 domain of Grb2. Under basal conditions, the SH3 domains of Grb2 direct the binding to the proline-rich carboxyl-terminal region of SOS. Thus, growth factor-stimulated tyrosine phosphorylation of Shc results in the formation of an Shc-Grb2-SOS ternary complex. Although the subcellular localization of this ternary complex has not been identified under all conditions, following epidermal growth factor stimulation Shc directs the association of the Grb2-SOS complex with the tyrosine-autophosphorylated epidermal growth factor receptor (36). Consequently, the targeting of SOS to the plasma membrane localizes SOS in close proximity to ras and thereby allows for the formation of a productive complex that mediates the guanylnucleotide exchange of GDP for GTP.

The above mechanism accounts for the rapid tyrosine kinase-mediated conversion of inactive ras to an active GTP-bound state. However, growth factor-activated ras (GTP bound) returns to the basal inactive GDP-bound state typically within 60 min following hormone stimulation (35). The molecular basis for the transient nature of ras activation has not been addressed to date. In the present study, we have demonstrated that in two independent cell types (CHO-IR and 3T3-L1 adipocytes) the SOS-Grb2 complex begins to disassociate following 5 min of hormone stimulation, with complete disassociation by 30 min. This hormone-stimulated disassociation of SOS from Grb2 was detected in the immunoprecipitates of both αGrb2 and αSOS. This observation cannot be explained by the translocation of the SOS-Grb2 complex to an insoluble compartment following insulin stimulation since it was also demonstrated in vitro following the preparation of detergent cell extracts. In addition, there was no detectable disassociation of the Grb2-Shc or Grb2-dynamin complexes under the same conditions which resulted in the disassociation of Grb2 and SOS. Thus, the physical uncoupling of the SOS-Grb2 complex is therefore consistent with the typical time frame of ras activation-inactivation and may account for the termination of the ras signal.

Previously, several laboratories have established that SOS is constitutively associated with Grb2 in the unstimulated (basal) state. However, these studies did not detect any significant differences in the degree of SOS-Grb2 association following hormone stimulation since they were performed in cells treated with activating agents for only 2 to 5 min (8, 12, 40). Consistent with our data, 5 min was minimally sufficient to detect the mobility shift of SOS and disassociation from Grb2 in 3T3-L1 adipocytes. However, complete disassociation of the SOS-Grb2 complex was not observed until the cells were stimulated for 15 to 30 min. Thus, the data presented in this study are consistent with these previous studies and demonstrate that the uncoupling between SOS and Grb2 occurs as a time-dependent event.

SOS contains seven consensus MAP kinase phosphorylation

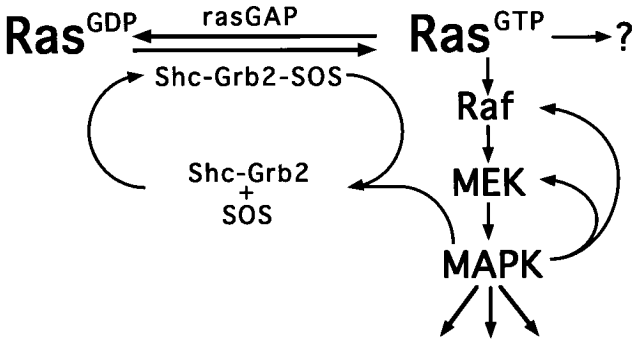


FIG. 10. Schematic model representating a proposed mechanism accounting for the transient activation of ras. The relative activation state of ras (GTP versus GDP bound) is determined by the activities of rasGAP and SOS. In this model, the tyrosine kinase receptor activation of ras occurs via the targeting of the SOS-Grb2 complex to tyrosine-phosphorylated Shc. Subsequent to ras activation, the raf1 kinase or related kinase becomes associated with GTP-bound ras and can then function to phosphorylate and activate a kinase cascade leading to activation of a MAP kinase (MAPK) family member(s). In turn, MAP kinase phosphorylates numerous proteins including MEK, raf, and perhaps SOS. The phosphorylation may be a necessary event in the disassociation of SOS from Grb2, thereby terminating the ras activation signal. In this manner, the MAP kinase phosphorylation of SOS could provide a feedback loop that results in a transient pattern of ras activation.

sites within the carboxyl-terminal proline-rich motif responsible for Grb2 SH3 binding (8, 12, 40, 44). In addition, several lines of evidence indicate that SOS is a direct substrate for MAP kinase activity. This includes in vitro phosphorylation of SOS by purified MAP kinase and the overexpression of MAP kinase, which results in a hypermobility shift of SOS (Fig. 2) (9, 49). Taken together, these observations suggest the presence of a potential MAP kinase feedback loop as illustrated in Fig. 10. Insulin-stimulated receptor tyrosine kinase activity results in the tyrosine phosphorylation of Shc. The association of SOS-Grb2 complexes with tyrosine-phosphorylated Shc leads to ras activation. This is presumably due to the appropriate targeting of SOS to ras, thereby initiating guanylnucleotide exchange of GTP for GDP. Once activated, ras couples to raf and in the presence of the raf-associated 14-3-3 proteins stimulates raf activity (13, 15, 21). In turn, activated raf phosphorylates and stimulates the kinase activity of the tyrosine/threonine-specific kinase MEK. MEK then directly phosphorylates MAP kinase, leading to its subsequent activation and the phosphorylation of MAP kinase substrates. Although our data demonstrate a relationship among the activation of the MAP kinase pathway, phosphorylation of SOS, and subsequent disassociation of the SOS-Grb2 complex, these data do not directly address which kinases are responsible for SOS phosphorylation. Since MAP kinase is one likely candidate, we speculate that a MAP kinase-dependent phosphorylation of SOS may be necessary for the disassociation of Grb2-SOS complexes, thereby terminating the ras activation signal and allowing rasGAP to convert GTP-bound ras to the inactive GDP-bound state.

This proposed feedback mechanism is analogous to the glucose regulation of adenylyl cyclase in *Saccharomyces cerevisiae* (18). In this pathway, the glucose signal is processed through the guanylnucleotide exchange factor Cdc25, which leads to the activation of ras and increased formation of intracellular cyclic AMP (cAMP). Subsequent activation of the cAMP-dependent protein kinase results in the phosphorylation and the disassociation of Cdc25 from the plasma membrane, thereby decreasing the exchange of GDP for GTP and reducing the level of ras activation.

In mammalian cells, there are several predictions and/or consequences of this proposed MAP kinase feedback pathway of ras regulation. Assuming that MAP kinase phosphorylation of SOS is the only event required for the uncoupling of the SOS-Grb2 complex, then any agent which increases MAP kinase activity should increase SOS phosphorylation and complex disassociation. This appears to be the case for several agents examined in this study including insulin, PDGF, TPA, and serum. In addition, following 48 h of v-*ras* or v-*raf* expression, a new steady state is reached with a partial serine/threonine-phosphorylated state of SOS. This partial phosphorylation of SOS results in a partial disassociation of the SOS-Grb2 complex. Furthermore, insulin stimulation of the v-*ras*- or v-*raf*-transfected cells augments the extent of SOS phosphorylation via a further increase in MAP kinase (data not shown) and induces a complete uncoupling of SOS-Grb2 binding. Since agents that activate MAP kinase (v-*ras*, v-*raf*, and TPA) independently of tyrosine kinase activity were also able to induce disassociation, the phosphorylation of SOS may be sufficient to uncouple the SOS-Grb2 complex.

Under this assumption, a reduction in the binding between SOS and Grb2 should also be reconstituted in vitro. In this regard, we have been able to demonstrate that a GST-Grb2 fusion protein can also detect the difference in SOS binding affinities from control and insulin-stimulated cells (Fig. 5 and 6A). However, we have not been able to demonstrate a difference in Grb2 binding to SOS following immunoprecipitation of SOS and incubation with purified GST-Grb2 protein (Fig. 6B). These data suggest that, although SOS phosphorylation is apparently necessary for the uncoupling of SOS-Grb2 interaction, it is not sufficient and another event may be required. The most likely explanation is the presence of an additional SOS-binding protein in the extracts from insulin-stimulated cells which was removed during the αSOS immunoprecipitation. Alternatively, it remains possible that, under the solid-phase conditions present in an immunoprecipitate, the antibody itself might perturb the interactions between SOS and Grb2, masking any affinity differences. Further studies will be necessary to clarify whether SOS phosphorylation per se is necessary and/or sufficient to induce the disassociation of the SOS-Grb2 complex.

Several studies have documented a feedback pathway whereby activation of the downstream MAP kinase phosphorylates the upstream kinases raf (1, 27) and MEK (31). The MAP kinase phosphorylation of raf inhibits raf kinase activity and thus provides an additional mechanism for the termination of MAP kinase signaling as well as the transient activation of MAP kinase activity (49). Since this pathway can effectively inactivate the MAP kinase cascade, there does not appear to be any specific cellular need to uncouple the SOS-Grb2 complex simply to terminate MAP kinase activation. We therefore speculate that the MAP kinase feedback mechanism responsible for the transient stimulation of ras is necessary in order to inhibit other parallel signaling pathways mediated by activated ras.

In summary, we have observed that growth factor stimulation of the ras signaling pathway and subsequent activation of MAP kinase generate a feedback pathway which results in the phosphorylation of SOS. The extent of this phosphorylation reaction parallels the uncoupling of the SOS-Grb2 complex without affecting the association of Grb2 with Shc or dynamin. The disassociation of SOS from Grb2 and, therefore, Shc may account for the transient activation of ras by removing the stimulatory signal for ras GTP loading. Further studies will be necessary to directly establish whether this is a direct consequence of MAP kinase-stimulated SOS phosphorylation and to

identify the physiological consequences of this event in the control of ras desensitization.


## ACKNOWLEDGMENTS

S.B.W. and K.Y. contributed equally to this study.

We thank Melanie Cobb for providing the MAP kinase, Bob Brown for help with cell culture, and Michael Czech for helpful discussions.

Support was provided by research grants DK33823 and KD25295 from the National Institutes of Health. S.B.W. was the recipient of a mentor-based postdoctoral fellowship award from the American Diabetes Association.


## ADDENDUM IN PROOF

After the submission of this article, Cherniak et al. (A. D. Cherniak, J. K. Klarlund, B. R. Conway, and M. P. Czech, J. Biol. Chem. **270:**1485–1488, 1995) also described in an insulin-stimulated disassociation of the SOS-Grb2 complex in 3T3L1 adipocytes.

## REFERENCES


1. **Anderson, N. G., P. Li, L. A. Marsden, N. Williams, T. M. Roberts, and T. W. Sturgill.** 1991. Raf-1 is a potential substrate for mitogen-activated protein kinase in vivo. Biochem. J. **277:**573–576.
2. **Aronheim, A., D. Engelberg, N. Li, N. Al-Alawi, J. Schlessinger, and M. Karin.** 1994. Membrane targeting of the nucleotide exchange factor Sos is sufficient for activating the Ras signaling pathway. Cell **78:**949–961.
3. **Avruch, J., X. F. Zhang, and J. M. Kyriakis.** 1994. Raf meets Ras: completing the framework of a signal transduction pathway. Trends Biochem. Sci. **19:**279–283.
4. **Baltensperger, K., L. M. Kozma, A. D. Cherniack, J. K. Klarlund, A. Chawla, U. Banerjee, and M. P. Czech.** 1993. Binding of the Ras activator Son of Sevenless to insulin receptor substrate-1 signaling complexes. Science **260:** 1950–1952.
5. **Blenis, J.** 1993. Signal transduction via the MAP kinases—proceed at your own RSK. Proc. Natl. Acad. Sci. USA **90:**5889–5892.
6. **Boulton, T. G., J. S. Gregory, and M. H. Cobb.** 1991. Purification and properties of extracellular signal-regulated kinase 1, an insulin-stimulated microtubule-associated protein 2 kinase. Biochemistry **30:**278–286.
7. **Bowtell, D., P. Fu, M. Simon, and P. Senior.** 1992. Identification of murine homologues of the Drosophila son of sevenless gene: potential activators of ras. Proc. Natl. Acad. Sci. USA **89:**6511–6515.
8. **Chardin, P., J. H. Camonis, N. W. Gale, L. Vanaelst, J. Schlessinger, M. H. Wigler, and D. Bar-Sagi.** 1993. Human Sos1—a guanine nucleotide exchange factor for Ras that binds to GRB2. Science **260:**1338–1343.
9. **Cherniak, A. D., J. K. Klarlund, and M. P. Czech.** 1994. Phosphorylation of the Ras nucleotide exchange factor Son of Sevenless by mitogen-activated protein kinase. J. Biol. Chem. **269:**4717–4720.
10. **Davis, R. J.** 1993. The mitogen-activated protein kinase signal transduction pathway. J. Biol. Chem. **268:**14553–14556.
11. **Draznin, B., L. Chang, W. J. Leitner, Y. Takata, and J. M. Olefsky.** 1993. Insulin activates p21Ras and guanine nucleotide releasing factor in cells expressing wild type and mutant insulin receptors. J. Biol. Chem. **268:**19998–20001.
12. **Egan, S. E., B. W. Giddings, M. W. Brooks, L. Buday, A. M. Sizeland, and R. A. Weinberg.** 1993. Association of Sos Ras exchange protein with Grb2 is implicated in tyrosine kinase signal transduction and transformation. Nature (London) **363:**45–51.
13. **Fantl, W. J., A. J. Muslin, A. Kikuchi, J. A. Martin, A. M. MacNicol, R. W. Gross, and L. T. Williams.** 1994. Activation of Raf-1 by 14-3-3 proteins. Nature (London) **371:**612–614.
14. **Frattali, A. L., J. L. Treadway, and J. E. Pessin.** 1991. Evidence supporting a passive role for the insulin receptor transmembrane domain in insulin-dependent signal transduction. J. Biol. Chem. **266:**9829–9834.
15. **Freed, E., M. Symons, S. G. Macdonald, F. McCormick, and R. Ruggieri.** 1994. Binding of 14-3-3 proteins to the protein kinase Raf and effects on its activation. Science **265:**1713–1716.
16. **Gibbs, J. B., M. S. Marshall, E. M. Scolnick, R. A. F. Dixon, and U. S. Vogel.** 1990. Modulation of guanine nucleotides bound to Ras in NIH3T3 cells by oncogenes, growth factors, and the GTPase activating protein (GAP). J. Biol. Chem. **265:**20437–20442.
17. **Gout, I., R. Dhand, I. D. Hiles, M. J. Fry, G. Panayotou, P. Das, O. Truong, N. F. Totty, J. Hsuan, G. W. Booker, I. D. Campbell, and M. D. Waterfield.** 1993. The GTPase dynamin binds to and is activated by a subset of SH3 domains. Cell **75:**25–36.
18. **Gross, E., D. Goldberg, and A. Levitzki.** 1992. Phosphorylation of the S. cerevisiae cdc25 in response to glucose results in its dissociation from Ras. Nature (London) **360:**762–765.
19. **Hashimoto, Y., K. Matuoka, T. Takenawa, K. Muroya, S. Hattori, and S. Nakamura.** 1994. Different interactions of Grb2/Ash molecule with the NGF and EGF receptors in rat pheochromocytoma PC12 cells. Oncogene **9:**869–875.
20. **Herskovits, J. S., H. S. Shpetner, C. C. Burgess, and R. B. Vallee.** 1993. Microtubules and src homology 3 domains stimulate the dynamin GTPase via its C-terminal domain. Proc. Natl. Acad. Sci. USA **90:**11468–11472.
21. **Irie, K., Y. Gotoh, B. M. Yashar, B. Errede, E. Nishida, and K. Matsumoto.** 1994. Stimulatory effects of yeast and mammalian 14-3-3 proteins on the Raf protein kinase. Science **265:**1716–1719.
22. **Keller, S. R., R. Aebersold, C. W. Garner, and G. E. Lienhard.** 1993. The insulin-elicited 160 kDa phosphotyrosine protein in mouse adipocytes is an insulin receptor substrate 1: identification by cloning. Biochim. Biophys. Acta **1172:**323–326.
23. **Keller, S. R., and G. E. Lienhard.** 1994. Insulin signalling: the role of insulin receptor substrate 1. Trends Cell Biol. **4:**115–119.
24. **Koide, H., T. Satoh, M. Nakafuku, and Y. Kaziro.** 1993. GTP-dependent association of Raf-1 with Ha-Ras—identification of Raf as a target downstream of Ras in mammalian cells. Proc. Natl. Acad. Sci. USA **90:**8683–8686.
25. **Lane, M. D., B. C. Reed, and P. R. Clements.** 1981. Insulin receptor synthesis and turnover in differentiating 3T3-L1 preadipocytes. Prog. Clin. Biol. Res. **66A:**523–542.
26. **Lee, C. H., W. Li, R. Nishimura, M. Zhou, A. G. Batzer, M. G. Myers, M. F. White, J. Schlessinger, and E. Y. Skolnik.** 1993. Nck associates with the SH2 domain-docking protein IRS-1 in insulin-stimulated cells. Proc. Natl. Acad. Sci. USA **90:**11713–11717.
27. **Lee, R., M. H. Cobb, and P. J. Blackshear.** 1992. Evidence that extracellular signal-regulated kinases are the insulin-activated Raf-1 kinase kinases. J. Biol. Chem. **267:**1088–1092.
28. **Li, N., A. Batzer, R. Daly, V. Yajnik, E. Y. Skolnik, P. Chardin, D. Bar-Sagi, B. Margolis, and J. Schlessinger.** 1993. Guanine-nucleotide-releasing factor hSos1 binds to Grb2 and links receptor tyrosine kinases to Ras signalling. Nature (London) **363:**85–88.
29. **Lowenstein, E. J., R. J. Daly, A. G. Batzer, W. Li, B. Margolis, R. Lammers, A. Ullrich, E. Y. Skolnik, and J. Schlessinger.** 1992. The SH2 and SH3 domain-containing protein GRB2 links receptor tyrosine kinases to ras signaling. Cell **70:**431–442.
30. **Martegani, E., M. Vanoni, R. Zippel, P. Coccetti, R. Brambilla, C. Ferrari, E. Sturani, and L. Alberghina.** 1992. Cloning by functional complementation of a mouse cDNA encoding a homologue of CDC25, a *Saccharomyces cerevisiae* RAS activator. EMBO J. **11:**2151–2157.
31. **Matsuda, S., Y. Gotoh, and E. Nishida.** 1993. Phosphorylation of *Xenopus* mitogen-activated protein (MAP) kinase kinase by MAP kinase kinase kinase and MAP kinase. J. Biol. Chem. **268:**3277–3281.
32. **Medema, R. H., and J. L. Bos.** 1993. The role of p21ras in receptor tyrosine kinase signaling. Crit. Rev. Oncog. **4:**615–661.
33. **Moodie, S. A., B. M. Willumsen, M. J. Weber, and A. Wolfman.** 1993. Complexes of RasGTP with Raf-1 and mitogen-activated protein kinase kinase. Science **260:**1658–1661.
34. **Myers, M. G., X. J. Sun, and M. F. White.** 1994. The IRS-1 signaling system. Trends Biochem. Sci. **19:**289–293.
35. **Nakafuku, M., T. Satoh, and Y. Kaziro.** 1992. Differentiation factors, including nerve growth factor, fibroblast growth factor, and interleukin-6, induce an accumulation of an active Ras-GTP complex in rat pheochromocytoma PC12 cells. J. Biol. Chem. **267:**19448–19454.
36. **Pelicci, G., L. Lanfrancone, F. Grignani, J. McGlade, F. Cavallo, G. Forni, I. Nicoletti, T. Pawson, and P. G. Pelicci.** 1992. A novel transforming protein (SHC) with an SH2 domain is implicated in mitogenic signal transduction. Cell **70:**93–104.
37. **Pronk, G. J., A. M. de Vries-Smits, L. Buday, J. Downward, J. A. Maassen, R. H. Medema, and J. L. Bos.** 1994. Involvement of Shc in insulin- and epidermal growth factor-induced activation of $p21^{ras}$. Mol. Cell. Biol. **14:** 1575–1581.
38. **Pronk, G. J., J. McGlade, G. Pelicci, T. Pawson, and J. L. Bos.** 1993. Insulin-induced phosphorylation of the 46- and 52-kDa Shc proteins. J. Biol. Chem. **268:**5748–5753.
39. **Quilliam, L. A., S. Y. Huff, K. M. Rabun, W. Wei, W. Park, D. Broek, and C. J. Der.** 1994. Membrane-targeting potentiates guanine nucleotide exchange factor CDC25 and SOS1 activation of ras transforming activity. Proc. Natl. Acad. Sci. USA **91:**8512–8516.
40. **Rozakis-Adcock, M., R. Fernley, J. Wade, T. Pawson, and D. Bowtell.** 1993. The SH2 and SH3 domains of mammalian Grb2 couple the EGF receptor to the Ras activator Msos1. Nature (London) **363:**83–85.
41. **Rozakis-Adcock, M., J. McGlade, G. Mbamalu, G. Pelicci, R. Daly, W. Li, A. Batzer, S. M. Thomas, J. Brugge, P. G. Pelicci, J. Schlessinger, and T. Pawson.** 1992. Association of the Shc and Grb2/Sem5 SH2-containing proteins is implicated in activation of the Ras pathway by tyrosine kinases. Nature (London) **360:**689–692.
42. **Shou, C., C. L. Farnsworth, B. G. Neel, and L. A. Feig.** 1992. Molecular cloning of cDNAs encoding a guanine-nucleotide-releasing factor for Ras p21. Nature (London) **358:**351–354.

43. **Simon, M. A., D. D. Bowtell, G. S. Dodson, T. R. Laverty, and G. M. Rubin.** 1991. Ras1 and a putative guanine nucleotide exchange factor perform crucial steps in signaling by the sevenless protein tyrosine kinase. Cell **67:** 701–716.
44. **Skolnik, E. Y., A. Batzer, N. Li, C. H. Lee, E. J. Lowenstein, M. Mohammadi, B. Margolis, and J. Schlessinger.** 1993. The function of GRB2 in linking the insulin receptor to Ras signaling pathways. Science **260:**1953–1955.
45. **Skolnik, E. Y., C. H. Lee, A. Batzer, L. M. Vicentini, M. Zhou, R. Daly, M. G. Myers, Jr., J. M. Backer, A. Ullrich, M. F. White, and J. Schlessinger.** 1993. The SH2/SH3 domain-containing protein GRB2 interacts with tyrosine-phosphorylated IRS-1 and Shc: implications for insulin control of ras signalling. EMBO J. **12:**1929–1936.
46. **Sun, X. J., D. L. Crimmins, M. G. Myers, M. Miralpeix, and M. F. White.** 1993. Pleiotropic insulin signals are engaged by multisite phosphorylation of IRS-1. Mol. Cell. Biol. **13:**7418–7428.
47. **Sun, X. J., P. Rothenberg, C. R. Kahn, J. M. Backer, E. Araki, P. A. Wilden, D. A. Cahill, B. J. Goldstein, and M. F. White.** 1991. Structure of the insulin receptor substrate IRS-1 defines a unique signal transduction protein. Nature (London) **352:**73–77.
48. **Trahey, M., and F. McCormick.** 1987. A cytoplasmic protein stimulates normal N-ras p21 GTPase, but does not affect oncogenic mutants. Science **238:**542–545.
49. **Ueki, K., S. Matsuda, K. Tobe, Y. Gotoh, H. Tamemoto, M. Yachi, Y. Akanuma, Y. Yazaki, E. Nishida, and T. Kadowaki.** 1994. Feedback regulation of mitogen-activated protein kinase kinase kinase activity of c-Raf-1 by insulin and phorbol ester stimulation. J. Biol. Chem. **269:**15756–15761.
50. **Wei, W., R. D. Mosteller, P. Sanyal, E. Gonzales, D. McKinney, C. Dasgupta, P. Li, B.-X. Liu, and D. Broek.** 1992. Identification of a mammalian gene structurally and functionally related to the CDC25 gene of *Saccharomyces cerevisiae*. Proc. Natl. Acad. Sci. USA **89:**7100–7104.
51. **White, M. F., R. Maron, and C. R. Kahn.** 1985. Insulin rapidly stimulates tyrosine phosphorylation of a Mr-185,000 protein in intact cells. Nature (London) **318:**183–186.
52. **Yamauchi, K., and J. E. Pessin.** 1994. Enhancement or inhibition of insulin signaling by insulin receptor substrate 1 is cell context dependent. Mol. Cell. Biol. **14:**4427–4434.
53. **Yonezawa, K., A. Ando, Y. Kaburagi, R. Yamamotohonda, T. Kitamura, K. Hara, M. Nakafuku, Y. Okabayashi, T. Kadowaki, Y. Kaziro, and M. Kasuga.** 1994. Signal transduction pathways from insulin receptors to Ras—analysis by mutant insulin receptors. J. Biol. Chem. **269:**4634–4640.
54. **Zhang, X. F., J. Settleman, J. M. Kyriakis, E. Takeuchisuzuki, S. J. Elledge, M. S. Marshall, J. T. Bruder, U. R. Rapp, and J. Avruch.** 1993. Normal and oncogenic P21 (ras) proteins bind to the amino-terminal regulatory domain of C-Raf-1. Nature (London) **364:**308–313.
55. **Zhou, S. Y., S. E. Shoelson, M. Chaudhuri, G. Gish, T. Pawson, W. G. Haser, F. King, T. Roberts, S. Ratnofsky, R. J. Lechleider, B. G. Neel, R. B. Birge, J. E. Fajardo, M. M. Chou, H. Hanafusa, B. Schaffhausen, and L. C. Cantley.** 1993. SH2 domains recognize specific phosphopeptide sequences. Cell **72:** 767–778.